

POLARONIC EFFECTS IN QUANTUM DOTS*

ASHOK CHATTERJEE AND SOMA MUKHOPADHYAY

School of Physics, University of Hyderabad
Hyderabad-500 046, India*(Received November 27, 2000)*

In this article we present the results of our investigations on the ground and the first excited states of a polaron in a polar semiconductor quantum dot in both two and three dimensions. We have also discussed the stability of a strong-coupling bipolaron in quantum dots. We have shown that below a critical value of the confinement length the bipolaron becomes unstable in a quantum dot and breaks up into two individual polarons. We have finally shown that the phonon-induced Zeeman splitting of the first excited level of a two-dimensional parabolic quantum dot becomes strongly size dependent below a certain size and decreases very rapidly with decreasing dot size.

PACS numbers: 68.65.+g, 71.38.+i

1. Introduction

With the recent advent of modern fabrication techniques such as molecular beam epitaxy, nanolithographic and etching techniques and selective ion implantation, the study of low dimensional systems has undergone a renaissance. It is now possible to realize ultra-small semiconductor structures with quantum confinement of carriers in all the spatial directions. These structures are typically of the order of a few nanometers in size and are commonly referred to as zero-dimensional objects or more technically as quantum dots.

Quantum dots contain a discrete number of electrons confined in a potential well which is generally referred to as the confining potential and possess discrete spectra of energy levels [1–3]. If the size of the dot (d) is smaller than the bulk Bohr exciton radius (a_B), the confinement is considered to be strong while the condition $d > a_B$ refers to the weak confinement regime [4].

* Presented at the XXIV International School of Theoretical Physics “Transport Phenomena from Quantum to Classical Regimes”, Ustroń, Poland, September 25–October 1, 2000.

Interest in the subject of quantum dots has continued unabated for more than a decade or so primarily for two reasons. First, it has an intrinsic appeal because the natural length scales involved in it are of the order of a few nanometers where the quantum effects show up in their full glory and therefore the issues of interest in the quantum dot problems are of fundamental nature from the point of view of basic physics. In fact, quantum dot systems can provide excellent grounds for testing quantum mechanics. Secondly, and perhaps more importantly, the quantum dot systems exhibit very many new physical effects which are very interesting and are also quite different from those of their bulk counterparts. Furthermore, quantum dot structures can be realized in both two and three dimensions and can also be fabricated in different shapes and sizes. This design flexibility and the novel physical effects make quantum dot structures technologically very promising in microelectronic devices which are ultrafast systems.

A quantum dot can be regarded as a giant atom and can hold many real atoms and has primarily two energy scales: the confinement energy and the repulsive Coulomb energy. As the size of an atom increases, the differences in the energy levels due to confinement decrease faster than the Coulomb energy. Therefore, it is expected that electron–electron interaction will be more important in a quantum dot than in a small natural atom [3]. In a quantum dot both the valence band and the conduction band have discrete energy levels. The valence band maximum can be called as the Highest Occupied Molecular Orbital (HOMO) and the conduction band minimum can be called as the Lowest Unoccupied Molecular Orbital (LUMO) and the HOMO–LUMO gap is the band gap which depends on the size of the quantum dot [4]. It turns out, quite expectedly, that various physical properties of a quantum dot depend on its size. For example, smaller sized nanocrystallites have higher intensity of luminescence and highly enhanced radiative rates. Another important feature of quantum dots is that in these systems surface effects are very important because the smaller the size of a dot, the larger is the proportion of atoms on the surface.

As we have already mentioned, in a quantum dot the electrons do not have any free directions. Furthermore, the de Broglie wavelength of the electrons is of the same length scale as the confinement length. If the confinement lengths of a quantum dot are of the same order in all the three directions, it is called a quasi-three-dimensional quantum dot or simply a three-dimensional (3D) quantum dot. If the confinement length in one particular direction (say z) happens to be much smaller as compared to those in the other two directions, then the resulting system is referred to as a quasi-two-dimensional quantum dot. Theoretically, sometimes a quasi-two-dimensional quantum dot is treated as a purely two-dimensional (2D) quantum dot for the sake of mathematical simplicity. This approximation would

be valid if the confinement length in the z -direction is extremely small which may be possible if the material is extremely thin in this direction. It turns out that the nature and details of the confining potential can be varied and one can have desired electronic energy spectra to a great extent. The reduced dimensionality with enormous design flexibility, the finite particle number and the presence of comparable energy scales have made this new area of mesoscopic systems extremely fascinating with lots of challenges and have opened up a new frontier in condensed matter research with tremendous potentiality to revolutionize technology.

2. Confining potential

A large number of experiments have been performed in the last few years to explore various physical properties of quantum dot structures to yield a wealth of data which have contributed to our understanding of these systems in a profound way. The optical experiments of Sikorski and Merkt [5] and Meurer *et al.* [6] on semiconductor quantum dots show that resonance frequencies are more or less independent of the number of electrons (N) in a dot which essentially implies that excitation spectrum of a quantum dot is not influenced by the electron–electron interaction. This seems to be a generalization of Kohn’s theorem [7] which states that the cyclotron frequency in a translationally invariant electron system is independent of the electron density and of the form of the electron–electron interaction. This theorem has been found valid for quantum dots in which the confinement potential is harmonic. We shall present here this generalized Kohn’s theorem which is due to Peeters [8]. Let us consider a 2D parabolic quantum dot with N electrons. The Hamiltonian of the system can be written as

$$H = H_0 + V \quad (2.1)$$

with

$$H_0 = \sum_{i=1}^N \frac{\vec{p}_i^2}{2m} + \frac{1}{2} \sum_{i=1}^N (\omega_x^2 x_i^2 + \omega_y^2 y_i^2) , \quad (2.2)$$

and

$$V = \sum_{i < j=1}^N u(\vec{r}_i - \vec{r}_j) , \quad (2.3)$$

where x_i and y_i are respectively the x and y component of the position vector \vec{r}_i of the i -th electron, \vec{p}_i is the momentum of the i -th electron, ω_x and ω_y are the frequencies of the confining parabolic potential in x and y directions,

respectively, and $u(\vec{r}_i - \vec{r}_j)$ represents the Coulomb interaction between the i -th and the j -th electrons. The noninteracting system described by H_0 can be diagonalized exactly and we get

$$H_0 = \hbar\omega_x \left(C_x^+ C_x^- + \frac{1}{2} \right) + \hbar\omega_y \left(C_y^+ C_y^- + \frac{1}{2} \right), \quad (2.4)$$

where

$$C_x^+ = \sum_{j=1}^N c_{j,x} = \sum_{j=1}^N \left(\frac{m\omega_x}{2\hbar} \right)^{1/2} \left(x_j - i \frac{p_{j,x}}{m\omega_x} \right), \quad (2.5)$$

$$C_x^- = \sum_{j=1}^N c_{j,x}^- = \sum_{j=1}^N \left(\frac{m\omega_x}{2\hbar} \right)^{1/2} \left(x_j + i \frac{p_{j,x}}{m\omega_x} \right), \quad (2.6)$$

and we have similar expressions for C_y^+ and C_y^- . The eigenfunctions $(\Psi_{n_x, n_y}^{(0)}(x, y))$ and eigenvalues $(E_{n_x, n_y}^{(0)})$ of H_0 are well-known.

We have

$$E_{n_x, n_y}^{(0)} = \hbar\omega_x \left(n_x + \frac{1}{2} \right) + \hbar\omega_y \left(n_y + \frac{1}{2} \right). \quad (2.7)$$

It is easy to prove that

$$[V, C_{x,y}^{\pm}] = 0 \quad (2.8)$$

for any V that depends only on the relative distance between any two particles. As a consequence of (2.8) we obtain

$$[H, C_{x,y}^{\pm}] = \pm \hbar\omega_{x,y} C_{x,y}^{\pm} \quad (2.9)$$

which implies that if Ψ_{n_x, n_y} is an eigenstate of H with energy E_{n_x, n_y} , then $C_x^{\pm} \Psi_{n_x, n_y}$ are also eigenstates of H with energies $E_{n_x, n_y} \pm \hbar\omega_x$ and $C_y^{\pm} \Psi_{n_x, n_y}$ are eigenstates with energies $E_{n_x, n_y} \pm \hbar\omega_y$. Thus one would conclude that the excitation spectrum of an interacting electron system in a 2D parabolic quantum dot consists of two sets of equidistant levels with separation equal to the bare harmonic oscillator frequencies ω_x, ω_y . In the presence of a uniform magnetic field B in the z -direction, we have to replace \vec{p}_i in (2.2) by $\vec{p}_i + \frac{e}{c} \vec{A}_i$, where \vec{A} is the vector potential. In the symmetric gauge, we take $\vec{A}_i = (-y_i, x_i, 0)B/2$. It is easy to show that H_0 can still be diagonalized. We get

$$H_0 = \hbar\omega_1 \left(D_1^+ D_1^- + \frac{1}{2} \right) + \hbar\omega_2 \left(D_2^+ D_2^- + \frac{1}{2} \right), \quad (2.10)$$

where

$$\omega_{1,2}^2 = \frac{1}{2} \left\{ (\omega_x^2 + \omega_y^2 + \omega_c^2) \pm \left[(\omega_x^2 + \omega_y^2 + \omega_c^2)^2 - 4\omega_x^2\omega_y^2 \right]^{1/2} \right\}, \quad (2.11)$$

$$D_{1,2}^\pm = \sum_{j=1}^N a_{1,2}^\pm(j), \quad (2.12)$$

$$\begin{aligned} a_{1,2}^\pm(j) = u_{1,2} \left\{ x_j \left(-\omega_{1,2}^2 + \omega_y^2 + \frac{1}{2}\omega_c^2 \right) \mp i \frac{p_{j,x}}{m\omega_{1,2}} \left(-\omega_{1,2}^2 + \omega_y^2 \right) \right. \\ \left. \mp iy_j \frac{\omega_c}{2\omega_{1,2}} \left(\omega_{1,2}^2 + \omega_y^2 \right) - \frac{p_{j,y}}{m} \omega_c \right\}, \end{aligned} \quad (2.13)$$

with

$$u_{1,2} = \left(\frac{m\omega_{1,2}}{2\hbar} \right)^{1/2} \left[(\omega_{1,2}^2 - \omega_y^2)^2 + \omega_c^2\omega_y^2 \right], \quad (2.14)$$

and

$$\omega_c = \frac{eB}{mc}. \quad (2.15)$$

One can easily verify that

$$[a_1^\pm(j), a_2^\pm(j)] = 0, \quad (2.16)$$

$$[a_s^-(j), a_s^+(j)] = 1, \quad \text{for } s = 1, 2. \quad (2.17)$$

Now again one can show that

$$[V, D_{1,2}^\pm] = 0, \quad (2.18)$$

so that we get

$$[H, D_{1,2}^\pm] = \pm \hbar \omega_{1,2} D_{1,2}^\pm. \quad (2.19)$$

Thus also in the presence of a magnetic field the separation of the energy levels of a system of interacting electrons in a parabolic quantum dot is identical to that in the absence of the Coulomb interaction. This seems to be true only for parabolic confinement. Therefore, the electron-number independent resonance frequencies obtained from optical measurements on semiconductor quantum dots imply that the confining potentials in these systems are almost parabolic.

3. Theoretical investigations

A large number of theoretical investigations on quantum dots have been reported in the literature in the last few years. One of the main aims of these studies has been to obtain the electronic energy spectrum. Several variational calculations have been performed to study the effect of confinement and Coulomb interactions. Maksym and Chakraborty [9] have investigated the role of electron–electron interaction in a quantum dot in a magnetic field by exact numerical diagonalization. They have obtained a rich structure in the electronic energy spectrum but the optical excitation energies of a parabolic quantum dot have indeed turned out to be the same as those of a single electron. This makes the interaction effects difficult to observe. Maksym and Chakraborty have however suggested that one should look for thermodynamic quantities which can show the electron–electron interaction effects. They have indeed calculated the specific heat which shows oscillations as a function of the magnetic field. The exact numerical diagonalization method is however computationally extensive and also suffers from the convergence problem. Approximate many body calculations based on Hartree method and Hartree–Fock method have also been performed [10]. Hartree method however neglects all correlations while Hartree–Fock method neglects Coulomb correlations.

Sometimes it is useful to consider instead of the actual problem a model problem which is simple enough to admit an exact solution but contains the essential features of the actual problem. Johnson and Payne [11] have made an attempt in this direction and their model calculation provides exact excitation spectra which show complex crossing as a function of the electron–electron interaction which is similar to the full numerical calculation. Later, several investigations [12] based on this exactly soluble model have also followed.

Besides electronic properties, the optical properties of quantum dots have also been studied by a number of authors. In fact recent years have witnessed a flurry of investigations in this area and a great deal of literature with extremely rich data has piled up.

4. Polaronic effects in quantum dots

A number of authors have studied the role of phonons and the effect of Electron-Longitudinal-Optical (LO) phonon interaction on various electronic properties of polar semiconductor quantum dots. Since most of the quantum dots available today are made of polar semiconductors, it would be natural to expect the formation of polarons in these systems. A polaron may be envisaged as a complex consisting of an electron together with the lattice distortion induced by it. Since the distortion of a lattice means exci-

tation of phonons, a polaron is essentially an electron dressed with a bunch of virtual phonons. In the present section we shall first present the model for the quantum dot polaron problem and then study the effect of polaronic interaction on the Ground State (GS) and the first Excited State (ES) energies of an electron in a parabolic quantum dot using a variational method. For the sake of generality we shall formulate the problem in N -dimensions and obtain results in two and three dimensional dots as special cases.

4.1. The model

The Hamiltonian for the N -Dimensional (N -D) symmetric parabolic Quantum Dot (QD) polaron problem can be written by generalizing the Fröhlich polaron Hamiltonian as

$$H' = H'_{\text{par}} + H'_{\text{ph}} + H'_{\text{ep}} \quad (4.1)$$

with

$$H'_{\text{par}} = -\frac{\hbar^2}{2m} \nabla_{\vec{r}'}^2 + \frac{1}{2} m \sum_{i=1}^N \omega_{pi}^2 x_i^2, \quad (4.2)$$

$$H'_{\text{ph}} = \hbar\omega_0 \sum_{\vec{q}'} b_{\vec{q}'}^\dagger b_{\vec{q}'}, \quad (4.3)$$

$$H'_{\text{ep}} = \sum_{q'} (\xi_{q'} e^{-i\vec{q}' \cdot \vec{r}'} b_{\vec{q}'}^\dagger + \text{h.c.}), \quad (4.4)$$

where all vectors are N -dimensional, $\vec{r}'(x'_1, x'_2 \dots x'_N)$ refers to the position vector of the electron, m is its Bloch effective mass, ω_{pi} is the frequency of the confining parabolic (harmonic) potential corresponding to the i -th direction, ω_0 is the LO phonon frequency which is assumed to be dispersionless, $b_{\vec{q}'}^\dagger (b_{\vec{q}'})$ is the creation (annihilation) operator for a longitudinal-optical phonon of wave vector \vec{q}' and $\xi_{\vec{q}'}$ is the electron-phonon interaction coefficient for which we shall use the prescription of Peeters *et al.* [13]. It is convenient to use the dimensionless Feynman units in which the energy is scaled by $\hbar\omega_0$, lengths are scaled by $r_0 = \left(\frac{\hbar}{m\omega_0}\right)^{1/2}$ and wave vectors by $q_0 = \left(\frac{m\omega_0}{\hbar}\right)^{1/2}$. This scaling is equivalent to putting $\hbar = m = \omega_0 = 1$. In Feynman units the Hamiltonian (4.1) reads

$$H = \frac{H'}{\hbar\omega_0} = H_{\text{par}} + H_{\text{ph}} + H_{\text{ep}}, \quad (4.5)$$

where

$$H_{\text{par}} = \frac{H'_{\text{par}}}{\hbar\omega_0} = -\frac{1}{2} \nabla_{\vec{r}'}^2 + \frac{1}{2} \sum_i \omega_i^2 x_i^2, \quad (4.5a)$$

$$H_{\text{ph}} = \frac{H'_{\text{ph}}}{\hbar\omega_0} = \sum_{\vec{q}} b_{\vec{q}}^{\dagger} b_{\vec{q}}, \quad (4.5b)$$

$$H_{\text{ep}} = \frac{H'_{\text{ep}}}{\hbar\omega_0} = \sum_{\vec{q}} (\xi_{\vec{q}} e^{-i\vec{q}\cdot\vec{r}} b_{\vec{q}}^{\dagger} + \text{h.c.}). \quad (4.5c)$$

In Eq. (4.5) everything is dimensionless, the dimensionless electron position vector $\vec{r}(x_1, x_2 \cdots x_N)$ and the phonon wave vector \vec{q} are given by

$$\vec{r} = \frac{\vec{r}'}{r_0}, \quad \vec{q} = \frac{\vec{q}'}{q_0}, \quad (4.6)$$

the dimensionless frequency ω_i of the confining potential is given by $\omega_i = \frac{\omega_{pi}}{\omega_0}$ and ξ_q is given by

$$\xi_q = \frac{\xi'_{q'}}{\hbar\omega_0} = i \left[\frac{\Gamma\left(\frac{N-1}{2}\right) 2^{(N-3/2)} \pi^{(N-1)/2}}{V_N q^{N-1}} \cdot \alpha \right]^{1/2}, \quad (4.7)$$

where V_N is the dimensionless volume of the N -dimensional dot and α is the dimensionless electron-phonon coupling constant. In what follows we shall consider a symmetric QD for which we have

$$\omega_{p1} = \omega_{p2} = \cdots = \omega_p, \quad (4.8)$$

or in dimensionless units

$$\omega_1 = \omega_2 = \cdots = \omega_N = \omega, \quad (4.9)$$

so that the Hamiltonian (4.5) becomes

$$H = -\frac{1}{2} \nabla_{\vec{r}}^2 + \frac{1}{2} \omega^2 r^2 + \sum_{\vec{q}} b_{\vec{q}}^{\dagger} b_{\vec{q}} + \sum_{\vec{q}} \left(\xi_{\vec{q}} e^{-i\vec{q}\cdot\vec{r}} b_{\vec{q}}^{\dagger} + \text{h.c.} \right). \quad (4.10)$$

4.2. The Lee-Low-Pines-Gross (LLPG) method

A number of approximate solutions of the Hamiltonian (4.10) have been reported in the literature in recent times (see [14] and references therein). We shall discuss here a variational technique[15] which is a modification of the canonical transformation method of Lee, Low and Pines [16] introduced first by Gross [17] in the free polaron problem and later used by Takeguhara and Kasuya [18] for the 3D bound polaron problem. This method admits a simple

and straight-forward generalization to N dimensions [19]. We shall therefore make an N -dimensional formulation and obtain results for $N = 2$ and $N = 3$ as special cases. We shall show that it is possible to extract using this method information about both the effective mass excited states and relaxed excited states [20]. In this method one first employs the transformation

$$U(\vec{r}) = \exp \left[\sum_{\vec{q}} \left\{ f_{\vec{q}}(\vec{r}) b_{\vec{q}}^{\dagger} - f_{\vec{q}}^*(\vec{r}) b_{\vec{q}} \right\} \right], \quad (4.11)$$

where $f_{\vec{q}}(\vec{r})$ is a function of both \vec{q} and \vec{r} and has to be obtained variationally. The Hamiltonian (4.10) then transforms into

$$\begin{aligned} \tilde{H} &= U^{-1} H U \\ &= \frac{1}{2} \left[\hat{\vec{p}}^2 + \sum_{\vec{q}} b_{\vec{q}}^{\dagger} \hat{\vec{p}} \cdot [\vec{p}, f_{\vec{q}}(\vec{r})] \right. \\ &\quad - \sum_{\vec{q}} b_{\vec{q}} \hat{\vec{p}} \cdot [\vec{p}, f_{\vec{q}}^*(\vec{r})] + \sum_{\vec{q}} b_{\vec{q}}^{\dagger} [\hat{\vec{p}}, f_{\vec{q}}(\vec{r})] \cdot \hat{\vec{p}} \\ &\quad - \sum_{\vec{q}} b_{\vec{q}} [\hat{\vec{p}}, f_{\vec{q}}^*(\vec{r})] \cdot \hat{\vec{p}} + \sum_{\vec{q}\vec{q}'} b_{\vec{q}}^{\dagger} b_{\vec{q}'}^{\dagger} [\hat{\vec{p}}, f_{\vec{q}}(\vec{r})] \cdot [\hat{\vec{p}}, f_{\vec{q}'}^*(\vec{r})] \\ &\quad - \sum_{\vec{q}\vec{q}'} b_{\vec{q}}^{\dagger} b_{\vec{q}'} [\hat{\vec{p}}, f_{\vec{q}}(\vec{r})] \cdot [\hat{\vec{p}}, f_{\vec{q}'}^*(\vec{r})] \\ &\quad - \sum_{\vec{q}\vec{q}'} b_{\vec{q}'} b_{\vec{q}}^{\dagger} [\hat{\vec{p}}, f_{\vec{q}}^*(\vec{r})] \cdot [\hat{\vec{p}}, f_{\vec{q}}(\vec{r})] \\ &\quad \left. + \sum_{\vec{q}\vec{q}'} b_{\vec{q}} b_{\vec{q}'} [\hat{\vec{p}}, f_{\vec{q}}^*(\vec{r})] \cdot [\hat{\vec{p}}, f_{\vec{q}'}(\vec{r})] \right] + \frac{1}{2} \omega^2 r^2 \\ &\quad + \sum_{\vec{q}} (b_{\vec{q}}^{\dagger} + f_{\vec{q}}^*(\vec{r})) (b_{\vec{q}} + f_{\vec{q}}(\vec{r})) \\ &\quad + \sum_{\vec{q}} \left\{ \xi_{\vec{q}} e^{-i\vec{q} \cdot \vec{r}} (b_{\vec{q}}^{\dagger} + f_{\vec{q}}^*(\vec{r})) + \text{h.c.} \right\}, \end{aligned} \quad (4.12)$$

where $\hat{\vec{p}} = -i\nabla_{\vec{r}}$ and we have used the condition

$$\sum_{\vec{q}} \left[f_{\vec{q}}^*(\vec{r}) \vec{\nabla} f_{\vec{q}}(\vec{r}) - f_{\vec{q}}(\vec{r}) \vec{\nabla} f_{\vec{q}}^*(\vec{r}) \right] = 0 \quad (4.13)$$

which implies that the current due to the displacement of the phonon field is zero in the confined state. The LLPG variational energy is now written as

$$E^{ND} = \langle 0 | \langle \Phi^{ND}(\vec{r}) | \tilde{H} | \Phi^{ND}(\vec{r}) \rangle | 0 \rangle, \quad (4.14)$$

where $|0\rangle$ is the unperturbed zero-phonon state and $\Phi^{ND}(\vec{r})$ is a real function of the electronic coordinates. Variation of E^{ND} with respect to $f_q^*(\vec{r})$ gives

$$\left\{ \left[\frac{\hat{p}^2}{2}, f_{\vec{q}}(\vec{r}) \right] + f_{\vec{q}}(\vec{r}) \right\} \Phi^{ND}(\vec{r}) = -\xi_q e^{-i\vec{q}\cdot\vec{r}} \Phi^{ND}(\vec{r}) \quad (4.15)$$

which has to be solved to obtain $f_q(\vec{r})$. Eq. (4.10) now reduces to

$$\begin{aligned} E^{ND} = & -\langle \Phi^{ND}(\vec{r}) | \frac{1}{2} \nabla^2 | \Phi^{ND}(\vec{r}) \rangle + \frac{1}{2} \omega^2 \langle \Phi^{ND}(\vec{r}) | r^2 | \Phi^{ND}(\vec{r}) \rangle \\ & + \frac{1}{2} \sum_{\vec{q}} \left\{ \xi_q^* \langle \Phi^{ND}(\vec{r}) | e^{i\vec{q}\cdot\vec{r}} f_{\vec{q}}(\vec{r}) | \Phi^{ND}(\vec{r}) \rangle + \text{h.c.} \right\}. \end{aligned} \quad (4.16)$$

To make further progress, we choose Φ^{ND} to be the eigenfunction of a trial Hamiltonian H_t *i.e.*

$$\begin{aligned} H_t \Phi_j^{ND}(\vec{r}) &= \left[\frac{\hat{p}^2}{2} + V_t(\vec{r}) \right] \Phi_j^{ND}(\vec{r}) \\ &= E_j^{ND} \Phi_j^{ND}(\vec{r}). \end{aligned} \quad (4.17)$$

It then follows from Eq. (4.16) that

$$f_{\vec{q}}(\vec{r}) \Phi_j^{ND}(\vec{r}) = - \sum_{j'} \frac{\langle \Phi_{j'}^{ND} | \xi_q e^{-i\vec{q}\cdot\vec{r}} | \Phi_j^{ND} \rangle}{(E_{j'}^{ND} - E_j^{ND} + 1)} | \Phi_{j'}^{ND} \rangle. \quad (4.18)$$

It then follows from Eq. (4.16) and (4.17) that

$$\begin{aligned} E_j^{ND} = & \langle \Phi_j^{ND} | \left(-\frac{1}{2} \nabla_{\vec{p}}^2 + \frac{1}{2} \omega^2 r^2 \right) | \Phi_j^{ND} \rangle \\ & - \sum_{\vec{q}} \sum_{j'} \frac{\left| \langle \Phi_{j'}^{ND} | \xi_q e^{-i\vec{q}\cdot\vec{r}} | \Phi_j^{ND} \rangle \right|^2}{(E_{j'}^{ND} - E_j^{ND} + 1)}. \end{aligned} \quad (4.19)$$

In what follows we shall make a harmonic oscillator potential approximation *i.e.* we choose the trial potential as $V_t(\vec{r}) = \frac{1}{2} \mu^4 r^2$. Then $\Phi_j^{ND}(\vec{r})$ and E_j^{ND} are given by

$$\begin{aligned} \Phi_j^{ND}(\vec{r}) = & \left(\frac{\mu^N}{\pi^{N/2} 2^{j_1+j_2+\dots+j_N} j_1! j_2! \dots j_N!} \right)^{1/2} \\ & \times H_{j_1}(\mu x_1) H_{j_2}(\mu x_2) \dots H_{j_N}(\mu x_N) e^{-\frac{\mu^2}{2} r^2}, \end{aligned} \quad (4.20)$$

$$E_j^{ND} = (j_1 + j_2 + \dots + j_N + \frac{N}{2}) \mu^2, \quad (4.21)$$

where $H_{ji}(\mu x_i)$ is a Hermite polynomial. The LLPG expressions for the ground and the first excited states are then finally given by

$$\begin{aligned}
 E_{\text{GS}}^{\text{ND}} &= \frac{N}{4z} + \frac{Nz}{4l^4} - \frac{\alpha\sqrt{\pi}}{2} \frac{\Gamma(\frac{N-1}{2})}{\Gamma(\frac{N}{2})} \frac{1}{\sqrt{z}} \frac{\Gamma(z+1)}{\Gamma(z+\frac{1}{2})}, \\
 E_{\text{ES}}^{\text{ND}} &= \frac{N+2}{4}\mu^2 + \left(\frac{N+2}{4l^4}\right) \frac{1}{\mu^2} - \frac{\alpha}{4N}\mu \frac{\Gamma(\frac{N-1}{2})}{\Gamma(\frac{N}{2})} \\
 &\quad \times \int_0^\infty dt e^{-(1-\mu^2)t} \left\{ \frac{(2N-1)e^{-\mu^2 t} + 1}{(1-e^{-\mu^2 t})^{1/2}} - 1 \right\} + \frac{\alpha}{4} \frac{\Gamma(\frac{N-1}{2})}{N\Gamma(\frac{N}{2})} \frac{\mu}{(\mu^2-1)},
 \end{aligned} \tag{4.22}$$

$$\tag{4.23}$$

where $z = \frac{1}{(\mu^2)}$ and l is the dimensionless confinement length which is given by $l = \frac{l_0}{r_0} = \frac{1}{\sqrt{\omega}}$ where l_0 and r_0 are defined as $l_0 = \left(\frac{\hbar}{m\omega_h}\right)^{1/2}$ and $r_0 = \left(\frac{\hbar}{m\omega_0}\right)^{1/2}$.

The polaronic correction (ΔE) to the ground state electron energy is defined as

$$\Delta E_{\text{GS}} = E_{\text{GS}}^{\text{ND}} - \frac{N}{2l^2},$$

where $E_{\text{GS}}^{\text{ND}}$ has to be obtained by minimizing (4.22) with respect to z for $N = 2$ and $N = 3$. In Figs. 1 and 2 we plot $(-\Delta E)$ as a function of l_0 for a few selected quantum dots of polar semiconductors such as InSb, GaAs, CdTe, CdSe and CdS. The material parameters used in the calculation have been taken from Ref. [21]. In Fig. 1 we show the behaviour for the 3D dots while the corresponding results for the 2D dots are plotted in Fig. 2. It is clear that polaronic effects increase with decreasing dot size and can become extremely large if the dot-size is reduced below a few nanometers. Furthermore, the polaronic effects are found in all cases stronger in 2D dots than in the corresponding 3D dots. For example, in the case of 3D CdS dot, $\Delta E = -22.29$ meV, for $l_0 = 40$ Å while for the corresponding 2D dot, $\Delta E = -35.13$ meV for the same value of l_0 . Furthermore, as the confinement length is reduced from 40 Å to 20 Å, the decrease in ΔE in the case of 3D CdS dot is -28.25 meV while that in the corresponding 2D case is -44.7 meV.

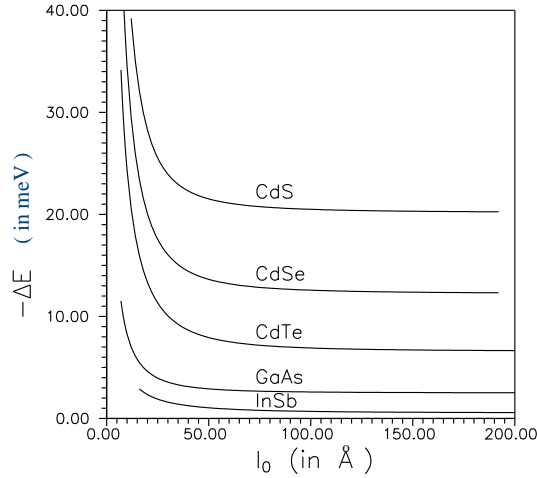


Fig. 1. Polaronic corrections, $-\Delta E$ (in meV) to the GS energy of an electron in InSb, GaAs, CdTe, CdSe and CdS quantum dots with parabolic confinement in 3D, as a function of the confinement length l_0 (in Å).

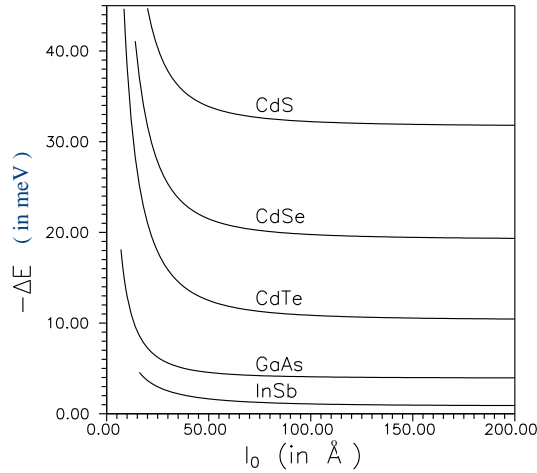


Fig. 2. Polaronic corrections, $-\Delta E$ (in meV) to the GS energy of an electron in InSb, GaAs, CdTe, CdSe and CdS quantum dots with parabolic confinement in 2D as a function of the confinement length l_0 (in Å).

The first excited state polaron energies for $N = 2$ and $N = 3$ have to be obtained by minimizing (4.23) with respect to μ . It may be noted that the energy expression (4.23) has a singularity at $\mu = 1$ corresponding to the instability of the excited state with respect to the emission of a phonon.

In the extended state limit *i.e.* for $l \rightarrow \infty$ and $\alpha \rightarrow 0$, we obtain

$$E_{\text{ES}}^{\text{ND}} = \left(\frac{N+2}{4} \right) \mu^2 + \left(\frac{N+2}{4l^4} \right) \frac{1}{\mu^2} - \frac{\alpha\sqrt{\pi}}{2} \frac{\Gamma(\frac{N-1}{2})}{\Gamma(\frac{N}{2})} \left[1 + \frac{(N+2)}{8N} \mu^2 \right] \quad (4.24)$$

which on minimization with respect to μ yields

$$\mu^2 = \frac{1}{l^2 \left[1 - \frac{\alpha\sqrt{\pi}}{4N} \frac{\Gamma(\frac{N-1}{2})}{\Gamma(\frac{N}{2})} \right]^{1/2}}. \quad (4.25)$$

Substituting Eq. (4.25) in (4.24) gives

$$E_{\text{ES,EMES}}^{\text{ND}} = -\frac{\alpha\sqrt{\pi}\Gamma(\frac{N-1}{2})}{2\Gamma(\frac{N}{2})} + \left(\frac{N+2}{2} \right) \frac{1}{l^2} \left[1 - \frac{\alpha\sqrt{\pi}\Gamma(\frac{N-1}{2})}{4N\Gamma(\frac{N}{2})} \right]^{1/2} \quad (4.26)$$

which is the Effective Mass Excited State (EMES) result. Since the first ES energy has a singularity at $\mu = 1$, the minima corresponding to the effective mass excited state would occur on the left side of the singularity. The situation described by Eq. (4.26) is that of an undisturbed weak-coupling polaron sitting at the first ES level of the confining parabolic potential of the quantum dot.

In the case of localised state limit *i.e.* for $\mu \rightarrow \infty$, we obtain

$$E_{\text{ES,Loc}}^{\text{ND}} = \left(\frac{N+2}{4} \right) \mu^2 + \left(\frac{N+2}{4l^4} \right) \frac{1}{\mu^2} - \frac{\alpha\Gamma(\frac{N-1}{2})}{2\Gamma(\frac{N}{2})} \times \left(1 - \frac{1}{4N} \right) \left(\frac{2 \ln 2 + \mu^2}{\mu} \right) \quad (4.27)$$

which on minimization with respect to μ yields

$$\left(\frac{N+2}{2} \right) \mu^4 - \left(\frac{N+2}{2} \right) \frac{1}{l^4} - \frac{\alpha}{2} \frac{\Gamma(\frac{N-1}{2})}{\Gamma(\frac{N}{2})} \left(1 - \frac{1}{4N} \right) (\mu^3 - 2\mu \ln 2) = 0. \quad (4.28)$$

In the limit of strong electron-phonon coupling and weak confinement, one can solve (4.28) approximately to obtain

$$\mu = \frac{\alpha}{N+2} \left(1 - \frac{1}{4N} \right) \frac{\Gamma(\frac{N-1}{2})}{\Gamma(\frac{N}{2})}. \quad (4.29)$$

Eq. (4.27) then reduces to

$$E_{\text{ES,RES}}^{\text{ND}} = -\frac{\alpha^2}{4(N+2)} \left(1 - \frac{1}{4N}\right)^2 \left(\frac{\Gamma(\frac{N-1}{2})}{\Gamma(\frac{N}{2})}\right)^2 + \frac{(N+2)^3}{4\alpha^2 l^4} \frac{1}{(1 - \frac{1}{4N})^2} \left\{\frac{\Gamma(N/2)}{\Gamma(\frac{N-1}{2})}\right\}^2 - (N+2) \ln 2 \quad (4.30)$$

which is the first relaxed excited state (RES) energy in the limit of large α and weak confinement. In the limit of strong confinement ($l \rightarrow 0$) and small electron-phonon coupling ($\alpha \rightarrow 0$), Eq. (4.28) can be approximately solved by dropping the third term to give

$$\mu^2 = \frac{1}{l^2}, \quad (4.31)$$

and thus in this limit the first RES energy is given by

$$E_{\text{ES,RES}}^{\text{ND}} = \frac{(N+2)}{2l^2} - \frac{\alpha}{2} \left(1 - \frac{1}{4N}\right) \frac{\Gamma(\frac{N-1}{2})}{\Gamma(\frac{N}{2})} \left(\frac{1}{l} + 2l \ln 2\right). \quad (4.32)$$

Since the first RES energy expressions (4.30) and (4.32) are obtained for large values of μ , the minima corresponding to these energies will be on the right side of the singularity. It may be mentioned that relaxed excited states occur when the localization potential for the electron arises from the combined effect of the lattice polarization and the confining parabolic potential.

The first ES polaronic correction to the quantum dot electron energy can be defined as

$$\Delta E_{\text{ES}} = E_{\text{ES}}^{\text{ND}} - \frac{N+2}{2l^2}$$

which as a function of μ would have in general two minima, one corresponding to the EMES which can occur for $\mu < 1$ and the other corresponding to the RES which can occur for $\mu > 1$. However for the excited polaronic states to exist, it is necessary that ΔE_{ES} is negative. We have studied the variation of ΔE_{ES} as a function of μ for both 2D and 3D dots for various sets of values of α and l . The typical behaviour is shown in Fig. 3 where we have taken $\alpha = 2$ and $l = 3$. It is evident that in 2D, ΔE_{ES} has only one minimum corresponding to the RES while in 3D, ΔE_{ES} has two minima, one corresponding to the EMES and the other to the RES, the EMES being, as expected, lower in energy. For $\alpha = 2$ and $l = 1$ we find that in both 2D and 3D, ΔE_{ES} shows only one minimum which occurs for $\mu > 1$ implying that the first excited states in these cases are of RES type. For $\alpha = 2$ and $l = 7$ we find that in 2D, ΔE_{ES} shows two minima, one giving the EMES energy

correction and the other giving the first RES energy correction. In 3D also we find that there are 2 minima in the $\Delta E_{\text{ES}}-\mu$ curve, but the minimum for $\mu > 1$ gives a positive polaronic energy and is therefore not acceptable. For $\alpha = 0.5$ and $l = 5.0$ we find that the first ES is of EMES type in both 2D and 3D dots. It should however be pointed out that when the minimum of the $\Delta E_{\text{ES}}-\mu$ curve is very close to the singularity, the energies obtained are not very accurate and therefore in such cases even if we may obtain a small positive value for ΔE_{ES} , the RES may still possibly exist.

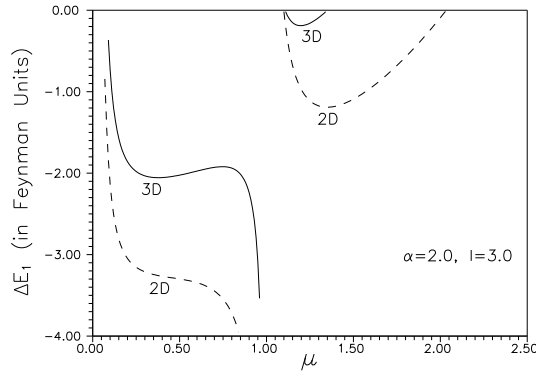


Fig. 3. Polaronic corrections, ΔE_{ES} (in Feynman units) to the ES energy of an electron in 2D and 3D quantum dots for $\alpha = 2$ and $l = 3$ as a function of the variational parameter μ .

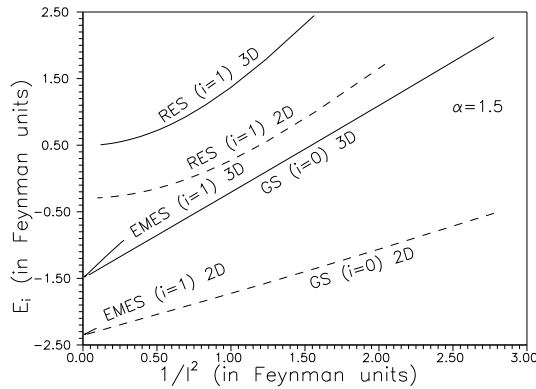


Fig. 4. EMES and RES energies (in Feynman units) of a polaron as a function of $1/l^2$ (in Feynman units) for $\alpha = 1.5$ in 2D and 3D quantum dots. The GS polaron energies are also shown for the sake of comparison.

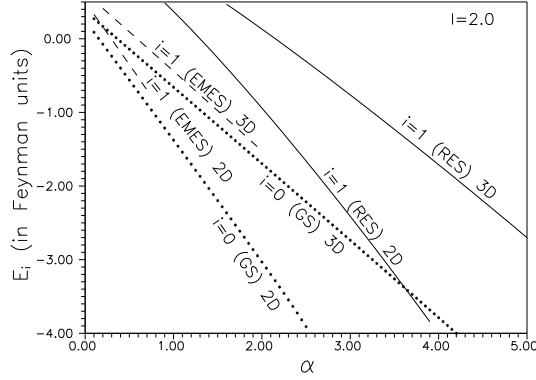


Fig. 5. EMES and RES energies (in Feynman units) of a polaron as a function of α for $l = 2$ in both 2D and 3D quantum dots. The GS energies are also shown for the sake of comparison.

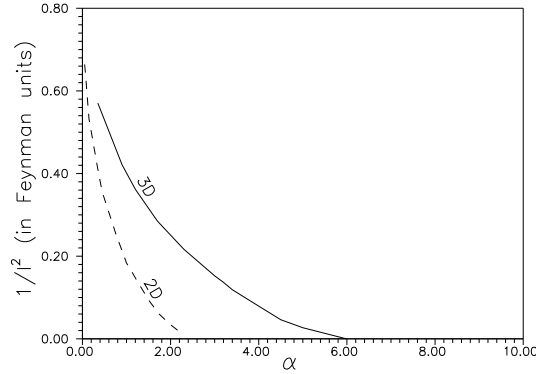


Fig. 6. The curve giving the critical values of α and $1/l^2$ (in Feynman units) below which EMES would exist in 2D and 3D quantum dots.

We have studied the behaviour of the EMES and the RES energies as a function of $\frac{1}{l^2}$ for $\alpha = 1.5$ in both two and three dimensions. The results are shown in Fig. 4 where we have also shown the behaviour of the GS polaron energy for the sake of comparison. In Fig. 5 we plot E_{GS} , E_{ES}^{EMES} and E_{ES}^{RES} as a function of α for $l = 2$ for both 2D and 3D dots. It is evident from all these figures that the difference between the GS energy and the first RES energy is always greater than an LO-phonon energy. It can also be noticed that for a particular value of α the EMES ceases to exist below a certain value of the confinement length l . Again for a given value of l the EMES exists only if α does not exceed a particular value. We show this behaviour more elaborately in Fig. 6 for both 2D and 3D dots. The points lying on the 2D and 3D curves correspond to the critical values of α and $\frac{1}{l^2}$ below

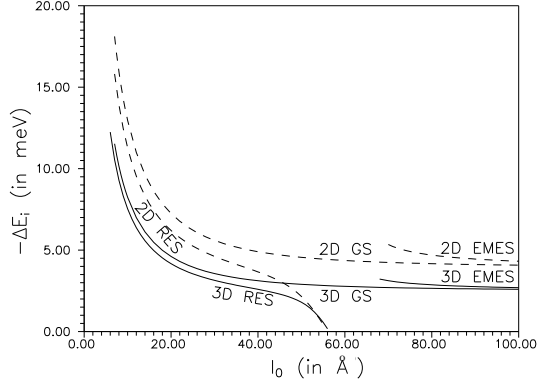


Fig. 7. Polaronic corrections, $-\Delta E_{ES}$ (in meV) to the ES energy of an electron in 2D and 3D GaAs quantum dots as a function of the confinement length l_0 (in Å). The GS energies are also shown for the sake of comparison.

which EMES would exist in the respective dimensions. Finally, we apply our results to realistic quantum dots. In Fig. 7 we show the behaviour of $-\Delta E_{ES}$ for 2D and 3D GaAs quantum dot. For the sake of comparison we have also plotted the GS polaronic energy corrections. It can be noticed that for large values of the confinement length the first ES of a polaron in a GaAs quantum dot is of the effective mass type. However, for a small dot the first ES of the polaron can be described by a relaxed excited state.

5. Formation and stability of a singlet optical bipolaron in a parabolic quantum dot

In the present section we investigate the formation and stability of a singlet optical bipolaron in 2D and 3D parabolic quantum dots in strong electron–phonon coupling region. We choose to work in the strong electron–phonon coupling regime because it is well-known that in bulk systems stable bipolarons form if α is larger than some critical value. The concept of the bipolaron was first introduced in the polaron literature by Pekar [22] in the early fifties and various aspects of the bipolaron have subsequently been investigated by several authors (see [23] and references therein). A bipolaron is a bound pair of two electrons dressed with a cloud of virtual phonons. Normally two conduction band electrons would repel each other because of their repulsive Coulomb interaction, but in polar materials there is an additional interaction between electrons mediated by virtual phonons which is attractive. If this phonon-mediated attractive interaction is large enough to overcome the mutual Coulomb repulsion then the electrons can form a bipolaronic bound state. The phenomenon of bipolaron formation is purely

of quantum origin since classically the net force between the two electrons is always repulsive, the effect of the electron-lattice polarization being merely to reduce the strength of the Coulomb repulsion by a factor $\varepsilon_0/\varepsilon_\infty$, where ε_0 and ε_∞ are respectively the static and high frequency dielectric constants. The bipolaron problem is interesting for both academic reasons and for its practical importance in polar semiconductors and semiconducting glasses. However, the discovery of high temperature superconductivity [24] in CuO_2 -based layer ceramic materials and the subsequent proposal of bipolaronic mechanism [25] for inducing pairing in these systems has made the bipolaron problem all the more fascinating and brought it to the forefront of current research.

It would also be interesting to explore the possibility of bipolaron formation in quantum dots. In [26] we have studied the stability of a strong-coupling optical bipolaron for the first time in two and three dimensional parabolic quantum dots using the Landau-Pekar variational method. Later the bipolaron problem in a quantum dot has also been studied by other authors [27]. In what follows we present our quantum dot bipolaron model [26] and then make an N -dimensional formulation for the bipolaron binding energy and finally discuss our numerical results.

5.1. The model

The Hamiltonian for a system of the two-electrons moving in an N -dimensional symmetric parabolic quantum dot and interacting with LO phonons of the system can be written as

$$\begin{aligned}
 H' = & -\frac{\hbar^2}{2m}\nabla_{\vec{r}'_1}^2 - \frac{\hbar^2}{2m}\nabla_{\vec{r}'_2}^2 + \frac{e^2}{\varepsilon_\infty|\vec{r}'_1 - \vec{r}'_2|} + \frac{1}{2}m\omega_p^2(r_1'^2 + r_2'^2) \\
 & + \hbar\omega_0 \sum_{\vec{q}'} b_{\vec{q}'}^\dagger b_{\vec{q}'} + \sum_{i=1}^2 \sum_{\vec{q}'} \left[\xi_{\vec{q}'}^i e^{-i\vec{q}' \cdot \vec{r}'_i} b_{\vec{q}'}^\dagger + \text{h.c.} \right], \quad (5.1)
 \end{aligned}$$

where again all vectors are N -dimensional. The first two terms refer to the kinetic energies of the two electrons, the third term describes their mutual Coulomb repulsion, the fourth term gives the potential energy of the two electrons due to the symmetric parabolic confinement, the fifth term describes the usual unperturbed phonon Hamiltonian, and the sixth term gives the interaction of the two electrons with the LO phonon field. In Feynman's units ($\hbar = \omega_0 = m = 1$) the Hamiltonian (5.1) reads

$$\begin{aligned}
H = & -\frac{1}{2}\nabla_{\vec{r}_1}^2 - \frac{1}{2}\nabla_{\vec{r}_2}^2 + \frac{\beta}{r_{12}} + \frac{1}{2}\omega^2(r_1^2 + r_2^2) + \sum_{\vec{q}} b_{\vec{q}}^\dagger b_{\vec{q}} \\
& + \sum_i \sum_{\vec{q}} \left[\xi_q e^{-i\vec{q}\cdot\vec{r}_i} b_{\vec{q}}^\dagger + \text{h.c.} \right], \quad (5.2)
\end{aligned}$$

where

$$\beta = \left(\frac{e^2}{\hbar\omega_0\epsilon_\infty} \right) / \left(\frac{\hbar}{m\omega_0} \right)^{1/2}. \quad (5.3)$$

5.2. Formulation

We seek a variational solution of (5.2) for a singlet bipolaron in the strong-coupling limit. In this limit the adiabatic approximation is valid and therefore we choose a trial wave function of the form

$$|\Psi_{\text{BP}}\rangle = |\Phi(\vec{r}_1, \vec{r}_2)\rangle \exp \left[\sum_{\vec{q}} (f_{\vec{q}} b_{\vec{q}}^\dagger - f_{\vec{q}}^* b_{\vec{q}}) \right] |0\rangle |\zeta\rangle, \quad (5.4)$$

where f_q 's are to be obtained variationally, $|0\rangle$ is the unperturbed zero-phonon state satisfying $b_{\vec{q}}|0\rangle = 0$ for all \vec{q} , $|\zeta\rangle$ is the antisymmetric spin function for the two electrons corresponding to the singlet pairing and $|\Phi(\vec{r}_1, \vec{r}_2)\rangle$ is a symmetric two-electron wave function. The variational energy (E_{BP}) is given by

$$\begin{aligned}
E_{\text{BP}} &= \langle \Psi | H | \Psi \rangle \\
&= -\frac{1}{2} \langle \Phi | \nabla_1^2 + \nabla_2^2 | \Phi \rangle + \sum_{\vec{q}} |f_{\vec{q}}|^2 + \langle \Phi | \frac{\beta}{r_{12}} | \Phi \rangle \\
&\quad + \frac{\omega^2}{2} \langle \Phi | r_1^2 + r_2^2 | \Phi \rangle + 2 \sum_{\vec{q}} (\xi_{\vec{q}} f_{\vec{q}}^* \rho_{\vec{q}}^* + \text{h.c.}), \quad (5.5)
\end{aligned}$$

where

$$\rho_{\vec{q}} = \langle \Phi | e^{i\vec{q}\cdot\vec{r}_i} | \Phi \rangle. \quad (5.6)$$

We choose the two-electron wave function as

$$|\Phi(\vec{r}_1, \vec{r}_2)\rangle = \phi(\vec{r}_1) \phi(\vec{r}_2) g(\vec{r}_1, \vec{r}_2, |\vec{r}_1 - \vec{r}_2|), \quad (5.7)$$

with ϕ as one-electron functions and g the Coulomb correlation factor. For $\phi(\vec{r})$ we try a Gaussian function and for the correlation factor g , we choose a Jastrow type function so that the normalised $\Phi(\vec{r}_1, \vec{r}_2)$ can be written as

$$|\Phi(\vec{r}_1 \vec{r}_2)\rangle = \left[\frac{\lambda^N (\lambda^2 - b)^{\frac{N}{2}+1}}{N \pi^N} \right]^{1/2} r_{12} \exp \left[-\frac{\lambda^2}{2} (r_1^2 + r_2^2) \right] \exp \left[\frac{b}{4} r_{12}^2 \right], \quad (5.8)$$

where λ and b are variational parameters. Variation of the energy E_{BP} with respect to f_q yields

$$f_q = -2\xi_q \rho_q, \quad (5.9)$$

where ρ_q is given by

$$\rho_q = \left[1 - \frac{q^2}{4N(\lambda^2 - b)} \right] \exp \left[-\frac{q^2}{8} \left\{ \frac{1}{\lambda^2} + \frac{1}{\lambda^2 - b} \right\} \right]. \quad (5.10)$$

We finally obtain for the bipolaron GS energy

$$\begin{aligned} E_{\text{BP}} = & \frac{N}{4} \lambda^2 + \frac{N}{4} t^2 \lambda^2 - \frac{1}{2} \left(1 - \frac{2}{N} \right) t^2 \lambda^2 + \frac{\sqrt{2} \beta \Gamma(\frac{N+1}{2}) t \lambda}{N \Gamma(\frac{N}{2})} \\ & + \frac{1}{4l^4} \left[\frac{N}{\lambda^2} + \frac{N+2}{\lambda^2 t^2} \right] - 2\sqrt{2} \frac{\Gamma(\frac{N-1}{2})}{\Gamma(\frac{N}{2})} (t^2 + 1)^{-1/2} t \lambda \alpha \\ & \times \left[1 - \frac{1}{N(t^2 + 1)} + \frac{3}{4N^2(t^2 + 1)^2} \right], \end{aligned} \quad (5.11)$$

where l is as usual the dimensionless effective confinement length and λ and t ($= \sqrt{\frac{\lambda^2 - b}{\lambda^2}}$) are variational parameters which have to be obtained numerically by solving the equations

$$\frac{\partial E_{\text{BP}}}{\partial \lambda} = 0 \quad \text{and} \quad \frac{\partial E_{\text{BP}}}{\partial t} = 0. \quad (5.12)$$

To obtain the stability criteria we have to find out the Binding Energy (BE) of the bipolaron which is given by

$$\text{BE} = 2E_p - E_{\text{BP}}, \quad (5.13)$$

where E_p is the GS energy of a single strong-coupling polaron in the same parabolic quantum dot system and should be calculated using the same approximation as were used for the determination of E_{BP} . E_p is given by

$$E_p = \frac{N}{4}\mu^2 + \frac{N}{4} \left(\frac{1}{l^4\mu^2} \right) - \frac{\alpha}{2} \frac{\Gamma(\frac{N-1}{2})}{\Gamma(\frac{N}{2})} \mu, \quad (5.14)$$

where μ has to be obtained numerically from

$$\frac{\partial E_p}{\partial \mu} = 0. \quad (5.15)$$

5.3. Numerical results and discussion

We determine the bipolaron stability by demanding that the binding energy of the bipolaron be positive. We find that binding energy of a strong-coupling bipolaron in a quantum dot depends on two parameters. These parameters are $\eta = \varepsilon_\infty/\varepsilon_0$ and the confinement length l .

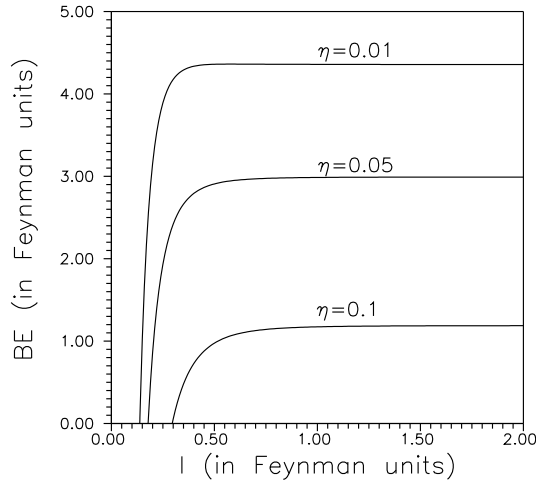


Fig. 8. Binding energy of the bipolaron (BE) (in Feynman units) as a function of the confinement length l (in Feynman units) for different values of η ($\eta = 0.01, 0.05, 0.1$) in a 3D quantum dot.

In Fig. 8 we show the variation of the bipolaron binding energy (BE) as a function of l for a few values of η ($\eta = 0.01, 0.05, 0.1$) for a 3D quantum dot. It is clear that the binding energy decreases with the decrease in the confinement length l . The variation is extremely rapid below a certain value of the confinement length and indeed the bipolaron becomes unstable if l is made smaller than a critical value l_c . At such confinement lengths a bipolaron breaks up into two individual polarons. This instability of the bipolaron

may be explained in the following way. As the effective confinement length of the quantum dot potential decreases, the average Coulomb repulsion between the two electrons increases. If this increase in the Coulomb repulsion with corresponding decrease in the size of the quantum dot becomes large enough to dominate over the phonon-mediated attractive electron–electron attraction, the formation of stable bipolarons will be inhibited. However, when l is large, the bipolaron binding energy does not change much with l and hence the bipolaron stability becomes more or less independent of l . This is essentially the bulk limit. It is also clear from the figure that the bipolaron binding energy increases with a decrease in η which is again not very difficult to understand. Since $\eta = (1 - \sqrt{2\frac{\alpha}{\beta}})$, for a given value of α , a decrease in η means a decrease in β and hence a reduction in the strength of the electron–electron Coulomb repulsion which in turn implies an increase in the electron–electron attractive interaction. Thus a decrease in η would lead to an enhancement in the bipolaron binding energy favouring the formation of stable bipolarons. The variation of the binding energy of the bipolaron with l for a 2D quantum dot is qualitatively similar to that observed in 3D dots and has not been shown here. Quantitatively however, the polaronic interactions are stronger in 2D than in 3D and consequently, for the same value of η , the bipolaron binding energy is found to be larger in a 2D dot than in 3D dot and also for a given value of η the critical confinement length l_e is smaller for a 2D quantum dot than for the corresponding 3D dot.

6. Phonon-induced suppression of Zeeman splitting in a polar quantum dot

In the preceding sections we have discussed the polaronic effects in quantum dots. It will, however, be important to calculate polaronic effects which can be easily measured experimentally and thus the existence or non-existence of these effects can be substantiated unambiguously. In a recent paper [28] we have made an attempt in this direction. The first excited level of a 2D parabolic quantum dot potential is two-fold degenerate. This two-fold degeneracy will be lifted in the presence of a magnetic field. This is the so called Zeeman effect in a parabolic quantum dot. It would be indeed interesting to study the effect of polaronic interaction on this Zeeman effect.

In recent times several authors [11,29] have studied the effect of a magnetic field on the electronic properties of a quantum dot. A few authors [30] have also addressed themselves to the problem of a quantum dot electron in a magnetic field in the presence of the electron-LO-phonon interaction. This is the so called magnetopolaron problem in a quantum dot. In [28] we have calculated the Zeeman splitting of the first excited level of a 2D polar semiconductor quantum dot with parabolic confinement in the presence of

an external magnetic field applied normal to the plane of the dot for small α using Rayleigh–Schrodinger perturbation theory (RSPT). An all coupling calculation has been performed by us in a subsequent work [31]. We shall present here the RSPT solution.

6.1. The model

The Hamiltonian for a magnetopolaron in a 2D quantum dot with symmetric parabolic confinement can be written as

$$\begin{aligned}
 H' = & \frac{1}{2m} \left(\vec{p}' + \frac{e\vec{A}'}{c} \right)^2 + \frac{1}{2} m \omega_p^2 \rho'^2 + \hbar \omega \sum_{\vec{q}'} b_{\vec{q}'}^\dagger b_{\vec{q}'} \\
 & + \sum_{\vec{q}'} \left[\xi_{\vec{q}'}' e^{-i\vec{q}' \cdot \vec{\rho}'} b_{\vec{q}'}^\dagger + \text{h.c.} \right], \quad (6.1)
 \end{aligned}$$

where all vectors are two dimensional, $\vec{\rho}'(x', y')$ and $\vec{p}' = -i\hbar\vec{\nabla}'$ are respectively the position vector and the momentum of the electron, e is the charge of the electron, \vec{A}' is the vector potential and other symbols have already been defined earlier. Let us consider that the magnetic field is applied in the z -direction and is of strength B *i.e.* we have $\vec{B} = (0, 0, B)$. We choose \vec{A}' such that $\vec{\nabla}' \cdot \vec{A}' = 0$ and work in the symmetric gauge so that \vec{A}' can be chosen as $\vec{A}' = (-\frac{1}{2}By', \frac{1}{2}Bx')$. Then the Hamiltonian (6.1) becomes

$$\begin{aligned}
 H' = & \frac{\vec{p}'^2}{2m} + \frac{eB}{2mc} (x'p_y' - y'p_x') + \frac{e^2 B^2}{8mc^2} \rho'^2 + \frac{1}{2} m \omega_p^2 \rho'^2 \\
 & + \hbar \omega_0 \sum_{\vec{q}'} b_{\vec{q}'}^\dagger b_{\vec{q}'} + \sum_{\vec{q}'} \left[\xi_{\vec{q}'}' e^{-i\vec{q}' \cdot \vec{\rho}'} b_{\vec{q}'}^\dagger + \text{h.c.} \right], \quad (6.2)
 \end{aligned}$$

or

$$\begin{aligned}
 H' = & \frac{\vec{p}'^2}{2m} + \frac{\omega_c'}{2} L_z' + \frac{1}{2} m \omega'^2 \rho'^2 + \hbar \omega_0 \sum_{\vec{q}'} b_{\vec{q}'}^\dagger b_{\vec{q}'} \\
 & + \sum_{\vec{q}'} \left(\xi_{\vec{q}'}' e^{-i\vec{q}' \cdot \vec{\rho}'} b_{\vec{q}'}^\dagger + \text{h.c.} \right), \quad (6.3)
 \end{aligned}$$

where $\omega_c' = \frac{eB}{mc}$ is the bare cyclotron frequency, $L_z' = (x'p_y' - y'p_x')$ is the z -component of the angular momentum of the electron, and $\omega' = (\omega_p^2 + \frac{\omega_c'^2}{4})^{1/2}$. We shall again use the Feynman units. The Hamiltonian (6.3) can then be written as

$$H = H_0 + H_{\text{ep}} = H_e + H_{\text{ph}} + H_{\text{ep}}, \quad (6.4)$$

with

$$H_e = -\frac{1}{2}\nabla_{\vec{\rho}}^2 + \frac{\omega_c}{2}L_z + \frac{1}{2}\bar{\omega}^2\rho^2, \quad (6.5)$$

$$H_{\text{ph}} = \sum_{\vec{q}} b_{\vec{q}}^\dagger b_{\vec{q}}, \quad (6.6)$$

$$H_{\text{ep}} = \sum_{\vec{q}} \left(\xi_{\vec{q}} e^{-i\vec{q}\cdot\vec{\rho}} b_{\vec{q}}^\dagger + \text{h.c.} \right), \quad (6.7)$$

where $\vec{\rho}(x, y) = \vec{\rho}'/r_0$, $\vec{q} = \vec{q}'/q_0$, $\omega = \omega_p/\omega_0$, $\omega_c = \omega'_c/\omega_0$, $\bar{\omega} = \omega'/\omega_0 = (\omega^2 + \frac{\omega_c^2}{4})^{1/2}$, $L_z = -i[x(\partial/\partial y) - y(\partial/\partial x)]$ and $|\xi_q|^2 = (\sqrt{2}\pi\alpha/V_2 q)V_2$ being the dimensionless area of the 2D dot. The Hamiltonian $H_0 = H_e + H_{\text{ph}}$ is exactly soluble. We are however interested in studying the effect of H_{ep} on the energy spectrum of H_0 . We shall obtain in particular the corrections to the GS and the first ES energies of H_0 due to H_{ep} . These may be referred to as the magnetopolaron self-energy corrections. In the subsection immediately following we shall calculate perturbatively the GS and the first ES magnetopolaron self energy corrections.

6.2. The RSPT solution

We have already mentioned that H_0 is exactly soluble. We have

$$H_0 \Psi_{nm}^{(0)}(\vec{\rho}) \prod_{\vec{q}} |n_q\rangle = \left(E_{nm}^{(0)} + \sum_{\vec{q}} n_q \right) \Psi_{nm}^{(0)}(\vec{\rho}) \prod_{\vec{q}} |n_q\rangle, \quad (6.8)$$

where

$$\sum_{\vec{q}} b_{\vec{q}}^\dagger b_{\vec{q}} \prod_{\vec{q}} |n_q\rangle = \left(\sum_{\vec{q}} n_{\vec{q}} \right) \prod_{\vec{q}} |n_q\rangle, \quad (6.9)$$

and

$$H_e \Psi_{nm}^{(0)}(\vec{\rho}) = E_{nm}^{(0)} \Psi_{nm}^{(0)}(\vec{\rho}). \quad (6.10)$$

We are interested in the perturbative effects of H_{ep} on the states $\Psi_{nm}^{(0)}(\vec{\rho})|0\rangle$ where $|0\rangle = \prod_q |0_q\rangle$. The wave functions $\Psi_{nm}^{(0)}(\vec{\rho})$ and the energy values $E_{nm}^{(0)}$ are given by

$$\Psi_{nm}^{(0)}(\vec{\rho}) = \frac{1}{\sqrt{2\pi}} e^{im\theta} \left(\frac{2\bar{\omega}n!}{(n+|m|)!} \right)^{1/2} (\sqrt{\bar{\omega}}\rho)^{|m|} L_n^{|m|}(\bar{\omega}\rho^2) e^{-\frac{\bar{\omega}}{2}\rho^2}, \quad (6.11)$$

$$E_{nm}^{(0)} = (2n + |m| + 1)\bar{\omega} + \frac{m}{2}\omega_c, \quad (6.12)$$

where $n = 0, 1, 2, \dots$, $m = 0, \pm 1, \pm 2, \dots$ and $L_n^{[m]}(\bar{\omega}\rho^2)$ is the associated Laguerre polynomial. In the absence of the magnetic field the first excited state $E_{0,\pm 1}^{(0)}$ is two-fold degenerate. This degeneracy is lifted in the presence of the magnetic field. This can be referred to as the Zeeman splitting in a parabolic quantum dot. We shall now study the effect of H_{ep} on this Zeeman splitting by the second-order RSPT.

The second-order RSPT correction to the energy of the state $\Psi_{nm}^{(0)}(\vec{\rho})|0\rangle$ due to the polaronic interaction is given by

$$\Delta E_{nm} = - \sum_{n'm'} \sum_{\{n_{\vec{q}'}\}} \frac{|\langle \Psi_{n'm'}^{(0)} | \prod_{\vec{q}'} \langle n_{\vec{q}'} | \left[\sum_{\vec{q}} \xi_{\vec{q}} e^{-i\vec{q} \cdot \vec{\rho}} b_{\vec{q}}^\dagger + \text{h.c.} \right] | \Psi_{nm}^{(0)} \rangle \prod_{\vec{q}'} |0_{\vec{q}'}\rangle|^2}{(E_{n'm'}^{(0)} + \sum_{\vec{q}'} n_{\vec{q}'} - E_{nm}^{(0)})}, \quad (6.13)$$

where $\sum_{\{n_{\vec{q}'}\}} = \sum_{n_{q_1}} \sum_{n_{q_2}} \sum_{n_{q_3}} \dots$. On further simplification (6.13) reduces to

$$\Delta E_{nm} = - \sum_{n'm'} \sum_{\vec{q}} \frac{|\langle \Psi_{n'm'}^{(0)}(\vec{\rho}) | \xi_{\vec{q}} e^{-i\vec{q} \cdot \vec{\rho}} | \Psi_{nm}^{(0)}(\vec{\rho}) \rangle|^2}{(E_{n'm'}^{(0)} - E_{nm}^{(0)} + 1)}. \quad (6.14)$$

Summation over \vec{q} in the above expression can be performed and we get

$$\Delta E_{nm} = - \frac{\alpha}{\sqrt{2}} \sum_{n'm'} \int \int \frac{d\vec{\rho} d\vec{\rho}'}{|\vec{\rho} - \vec{\rho}'|} \frac{|\langle \Psi_{n'm'}^{(o)*}(\vec{\rho}) \Psi_{n'm'}^{(0)}(\vec{\rho}') \Psi_{nm}^{*(o)}(\vec{\rho}') \Psi_{nm}^{(0)}(\vec{\rho}) \rangle|}{(E_{n'm'}^{(0)} - E_{nm}^{(0)} + 1)}. \quad (6.15)$$

Zhu and Gu (1993) [30] have also considered the same weak-coupling magnetopolaron problem but have restricted their study to the strong magnetic field limit. They have evaluated the energy expression by taking $n' = n$ and $m' = m$. One may notice that the infinite sum over n', m' occurring in equation (6.15) is the Green's function for the unperturbed electronic problem. For the magnetic field alone the corresponding Green's function was first derived by Sondheimer and Wilson [32] and for a magnetic field with a 3D harmonic oscillator potential it was first obtained by Lepine and Matz [33]. In the present case the unperturbed problem involves a 2D harmonic oscillator in a magnetic field. This Green's function can be obtained exactly for all values of the magnetic field for the ground state ($n = 0, m = 0$) and for small values of the magnetic field $[(\bar{\omega} + \frac{\omega_c}{2}) < 1]$ for the first two excited

states ($n = 0, m = \pm 1$). We obtain

$$\begin{aligned}
 G_{nm}(\vec{\rho}, \vec{\rho}') &= \sum_{n'm'} \frac{\Psi_{n'm'}^*(\vec{\rho}) \Psi_{n'm'}(\vec{\rho}')}{E_{n'm'}^{(0)} - E_{nm}^{(0)} + 1} \\
 &= \int dt e^{-(1-E_{nm}^{(0)})t} \frac{\bar{\omega}}{2\pi \sinh(\bar{\omega}t)} \\
 &\quad \times \exp \left[-\frac{\bar{\omega}}{2} \left\{ (\rho^2 + \rho'^2) \coth \bar{\omega}t - 2\vec{\rho} \cdot \vec{\rho}' \frac{\cosh(\omega_c t/2)}{\sinh(\bar{\omega}t)} \right. \right. \\
 &\quad \left. \left. - 2i(x'y - y'x) \frac{\sinh(\frac{\omega_c t}{2})}{\sinh(\bar{\omega}t)} \right\} \right]. \tag{6.16}
 \end{aligned}$$

Substituting (6.16) in (6.15) and performing integrations over $\vec{\rho}$ and $\vec{\rho}'$ we finally get

$$E_{nm} = E_{nm}^{(0)} + \Delta E_{nm}, \tag{6.17}$$

where E_{nm} is the perturbed energy and

$$\Delta E_{00} = -\frac{\alpha\sqrt{\pi}\sqrt{\bar{\omega}}}{2} \int_0^\infty dt \frac{e^{-t}}{[1 - e^{-\bar{\omega}t} \cosh(\frac{\omega_c t}{2})]^{1/2}}, \tag{6.18}$$

and

$$\Delta E_{0,\pm 1} = \frac{-\alpha\sqrt{\pi}\sqrt{\bar{\omega}}}{\sqrt{2}} \int_0^\infty dt \frac{e^{-[1-\bar{\omega} \mp \frac{\omega_c}{2}]t} [2f(g \mp h) + h^2 - f^2]}{(1 - e^{-2\bar{\omega}t}) [f(gf + h^2)]^{3/2}}, \tag{6.19}$$

where

$$f = 1 + \coth(\bar{\omega}t) - \cosh(\omega_c t/2)/\sinh(\bar{\omega}t), \tag{6.20}$$

$$g = 1 + \coth(\bar{\omega}t) + \cosh(\omega_c t/2)/\sinh(\bar{\omega}t), \tag{6.21}$$

and

$$h = \frac{\sinh(\frac{\omega_c t}{2})}{\sinh(\bar{\omega}t)}. \tag{6.22}$$

It may be noted that results (6.18) and (6.19) are exact to order α .

We define the renormalized cyclotron frequencies as $\omega_{c\pm}^* = (E_{0,\pm 1} - E_{00})/\hbar$ and the corresponding cyclotron masses as $m_{\pm}^* = m(\omega_c/\omega_{c\pm}^*)$. It is possible to obtain simple analytical expressions for the magnetopolaron self-energy corrections in different limiting cases. However, we shall present here our numerical results for a GaAs quantum dot.

6.3. Numerical results

We have already pointed out that the two-fold degeneracy of the first excited level of a 2D parabolic quantum dot potential is lifted in the presence of a magnetic field. Consequently, the bare cyclotron frequency ω_c splits into two cyclotron frequencies ω_{c+}^* and ω_{c-}^* . With increasing magnetic field ω_{c+}^* increases while ω_{c-}^* decreases. We have studied the behaviour of the renormalised cyclotron resonance frequencies ω_{c+}^* and ω_{c-}^* as a function of ω_c' in a GaAs quantum dot incorporating the electron-phonon interaction. We have found that when the polaronic interaction is taken into account the cyclotron resonance frequencies decrease quite significantly and furthermore their variation with the magnetic field also becomes slower, more so for larger magnetic fields [28].

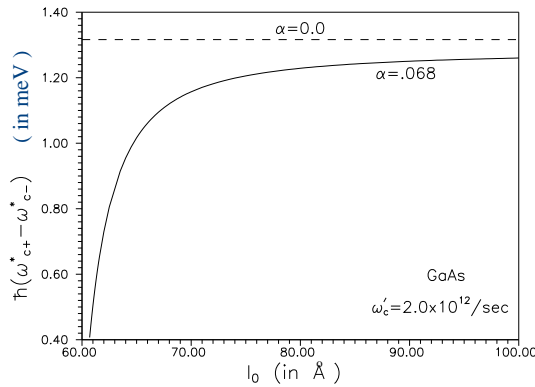


Fig. 9. Zeeman splitting (in meV) for a GaAs dot as a function of the confinement length (in Å) for a particular value of the magnetic field.

It is however more useful from the point of view of experimental observation to study the behaviour of the Zeeman splitting $[\hbar(\omega_{c+}^* - \omega_{c-}^*)]$ directly as a function of the dot size. Results are shown in Fig. 9. In the absence of any polaronic interaction the Zeeman splitting in a quantum dot is essentially independent of the confinement length, while for $\alpha = 0.068$, *i.e.* in a GaAs quantum dot it is found to be strongly size dependent below a certain value of l_0 . In fact, the Zeeman splitting decreases very rapidly with decreasing dot size below a few nanometers. This is a very interesting theoretical observation and should be experimentally measurable. For a bulk GaAs system also the Zeeman splitting is suppressed in the presence of the polaronic interaction but this suppression is independent of the system size. In a parabolic quantum dot of a polar semiconductor the excited unperturbed states $n = 0$, $m = \pm 1$, (plus zero phonon) strongly mix with the $n = 0$, $m = 0$ plus one phonon state resulting in the devaluation of the

axial angular momentum of the pure first excited states of the quantum dot potential. This explains the suppression of the Zeeman splitting in the presence of the electron–phonon interaction. It is now well known that when the confinement length becomes comparable to the polaron size, the polaronic effects become extremely pronounced and increase sharply with the decrease in the confinement length. Thus it is expected that in the presence of the polaronic interaction the Zeeman effect will be strongly suppressed if the effective dot size is reduced below a few nanometers. This interesting size dependence of Zeeman splitting in a parabolic quantum dot can be usefully exploited to obtain any desired resonant absorption in a GaAs quantum dot by tuning the frequency of the confining potential or the effective dot size.

7. Conclusion

In conclusion, we have shown that the polaronic corrections, ΔE to the electronic energy increase with decreasing confinement length l in both 2D and 3D quantum dots. We also find that for the same value of the electron–phonon coupling constant α and the confinement length l the polaronic effects are more pronounced in a 2D dot than in a 3D one. We have shown that the first excited polaronic states in a quantum dot can be of two types; one is EMES (effective mass excited state) and the other one can be referred to as RES (relax excited state). We find that in GaAs quantum dots the first excited states are of the EMES type if the dot sizes are large while for small dots the first excited states can be described by RES.

We have studied the stability of a strong-coupling optical bipolaron in two- and three-dimensional parabolic quantum dots and have shown that the bipolaron stability in these systems depends on two parameters, $\eta (= \varepsilon_\infty / \varepsilon_0)$ and l . The bipolaron binding energy decreases with the decrease in l and below a certain value of l which depends on η and the dimensionality of the dot, a bipolaron becomes unstable and breaks up into two individual polarons.

We have finally investigated the effect of the electron-LO-phonon interaction on the ground and the first excited states of a 2D parabolic quantum dot in the presence of an external magnetic field for small α . We find that below a certain value of l the Zeeman splitting becomes strongly size dependent and decreases very rapidly with decreasing dot size. This size-dependent suppression of the Zeeman splitting in a polar quantum dot is a clear manifestation of the quantum size effect and can have interesting technological applications.

REFERENCES

- [1] M.A. Kastner, *Phys. Today* **46**, 24 (1993).
- [2] N.F. Johnson, *J. Phys. Condens. Matter* **7**, 965 (1995).
- [3] R.C. Ashoori, *Nature* **379**, 413 (1996).
- [4] V.A. Singh, V. Ranjan, M. Kapoor, *Bull. Mater. Sci.* **22**, 563 (1999).
- [5] Ch. Sikorski, U. Merkt, *Phys. Rev. Lett.* **62**, 2164 (1989).
- [6] B. Meurer, D. Heitmann, K. Ploog, *Phys. Rev. Lett.* **68**, 1371 (1992).
- [7] W. Kohn, *Phys. Rev.* **123**, 1242 (1961).
- [8] F.M. Peeters, *Phys. Rev.* **B42**, 1486 (1990).
- [9] P.A. Maksym, T. Chakraborty, *Phys. Rev. Lett.* **65**, 108 (1990).
- [10] A. Kumar, S.E. Laux, F. Stern, *Phys. Rev.* **42**, 5166 (1990); V. Gudmundsson, R.R. Gerhardts, *Phys. Rev.* **B43**, 12098 (1991); D. Pfannkuche, V. Gudmundsson, P.A. Maksym, *Phys. Rev.* **B47**, 2244 (1993).
- [11] N.F. Johnson, M.C. Payne, *Phys. Rev. Lett.* **67**, 1157 (1991).
- [12] N.F. Johnson, *Phys. Rev.* **B46**, 2636 (1992); N.F. Johnson, M.C. Payne, *Phys. Rev.* **B45**, 3819 (1992); N.F. Johnson, *J. Phys. Condens. Matter* **4**, L555 (1992); N.F. Johnson, M. Reina, *J. Phys. Condens. Matter* **4**, L623 (1992).
- [13] F.M. Peeters, Wu Xiaoguang, J.T. Devreese, *Phys. Rev.* **B33**, 3926 (1986).
- [14] S. Mukhopadhyay, A. Chatterjee, *Phys. Lett.* **A204**, 411 (1995); *Phys. Lett.* **A240**, 100 (1998); *Phys. Lett.* **A242**, 355 (1998); *Int. J. Mod. Phys.* **B10**, 2781 (1996); *J. Phys. Condens. Matter* **11**, 2071 (1999); *Phys. Rev.* **B55**, 9279 (1997).
- [15] S. Mukhopadhyay, A. Chatterjee, *Phys. Rev.* **B58**, 2088 (1998).
- [16] T.D. Lee, F. Low, D. Pines, *Phys. Rev.* **90**, 297 (1953).
- [17] E.P. Gross, *Ann. Phys. (N.Y.)* **8**, 78 (1959).
- [18] K. Takeguhara, T. Kasuya, *J. Phys. Soc. Jpn.* **39**, 1292 (1975).
- [19] A. Chatterjee, *Ann. Phys. (N.Y.)* **202**, 320 (1990).
- [20] Y. Lepine, *Solid State Commun.* **52**, 427 (1984).
- [21] E. Kartheuser, in *Polaron in Ionic Crystals, Polar Semiconductors*, ed. J.T. Devreese, North Holland, Amsterdam 1972, p. 717.
- [22] S.I. Pekar, *Research on Electron Theory of Crystals*, Washington, DC: US AEC, 1963.
- [23] S. Sil, A. Chatterjee, *Int. J. Mod. Phys.* **B4**, 1879 (1990); S. Sil, A.K. Giri, A. Chatterjee, *Phys. Rev.* **B43**, A. Chatterjee, S. Sil, *Mod. Phys. Lett.* **B7**, 1071 (1993); A. Chatterjee, S. Sil, *Int. Mod. Phys.* **B7**, 4763 (1993).
- [24] J.G. Bednorz, K.A. Müller, *Z. Phys.* **B64**, 189 (1986).
- [25] A.S. Alexandrov, N.F. Mott, *Rep. Prog. Phys.* **57**, 1197 (1994) and references therein; D. Emin, *Phys. Rev. Lett.* **62**, 1544 (1989); B.K. Chakraverty, D. Feinberg, H. Zhen, M. Avignon, *Solid State Commun.* **64**, 1147 (1987); P. Prelovsek, T.M. Rice, F.C. Zhang, *J. Phys. C: Solid State Phys.* **20**, L229 (1987); A. Chatterjee, S. Sil, *Mod. Phys. Lett.* **B6**, 959 (1992).

- [26] S. Mukhopadhyay, A. Chatterjee, *J. Phys. Condens. Matter* **8**, 4017 (1996).
- [27] Y. Wan, G. Ortiz, P. Phillips, *Phys. Rev.* **B55**, 5313 (1997).
- [28] S. Mukhopadhyay, A. Chatterjee, *Phys. Rev.* **B59**, R7833 (1999).
- [29] V. Halonen, T. Chakraborty, P. Pietilainen, *Phys. Rev.* **B45**, 5980 (1992); U. Merkt, J. Huser, M. Wagner, *Phys. Rev.* **B43**, 7320 (1991); S.K. Yip, *Phys. Rev.* **B43**, 1707 (1991); Q.P. Li, K. Karrai, S.K. Yip, S. Das Sarma, H.D. Drew, *Phys. Rev.* **B43**, 5151 (1991); P.A. Maksym, T. Chakraborty, *Phys. Rev.* **B45**, 1951 (1992); S. Taut, *J. Phys. A: Math. Gen.* **27**, 1045 (1994); L. Quiroga, D. Aridila, N.F. Johnson, *Solid State Commun.* **89**, 661 (1994); R. Kotlyar, S. Das Sarma, *Phys. Rev.* **B55**, 5297 (1997); M. Dineykhon, R.G. Nazmitdimov, *Phys. Rev.* **B55**, 13707 (1997); S.C. Benjamin, N.F. Johnson, *Phys. Rev.* **B55**, R4903 (1997).
- [30] K.D. Zhu, S.W. Gu, *Phys. Rev.* **B47**, 12941 (1993); K.D. Zhu, T. Kobayashi, *Solid State Commun.* **92**, 353 (1994); Au-Yeung, K.D. Zhu, T. Kobayashi, *Solid State Commun.* **95**, 805 (1995); J.M. Ferreyra, P. Bosshard, C.R. Proettr, *Phys. Rev.* **B55**, 13682 (1997); Y. Lepine, G. Bruneau, *J. Phys. Condens. Matter* **10**, 1495 (1998); S.A. UcGill, K. Cao, W.B. Fowler, G.G. Deleo, *Phys. Rev.* **B57**, 8951 (1998).
- [31] S. Mukhopadhyay, A. Chatterjee, *Int. J. Mod. Phys. B*, in press.
- [32] E.H. Sondheimer, A.H. Wilson, *Proc. R. Soc. London*, **A210**, 173 (1952).
- [33] Y. Lepine, D. Matz, *Can. J. Phys.* **54**, 1979 (1976).